Statics and dynamics of worm-like surfactant micelles

REVIEW ARTICLE

Statics and dynamics of worm-like surfactant micelles

M E Cates† and S J Candau‡

† Cavendish Laboratory, Madingley Road, Cambridge CB3 0HE, UK
‡ Laboratoire de Spectrometrie et d'Imagerie Ultrasonores, Université Louis Pasteur, 4 rue Blaise Pascal, 67070 Strasbourg Cedex, France

Abstract. In certain surfactant solutions, such as aqueous cetyltrimethylammonium bromide (CTAB) in 0.1 M KBr, the amphiphiles are found to assemble reversibly into long, flexible worm-like micelles. Above a few per cent surfactant, these form an entangled viscoelastic fluid, reminiscent of a polymer solution. We review some recent experimental and theoretical progress concerning the equilibrium statistics and dynamics of these systems, which differ from normal polymer solutions in that the chains can break and reform reversibly.

1. Introduction

In dilute solutions, surfactant molecules can assemble reversibly into a variety of spatially organised structures. These include ordered phases (cubic, hexagonal, lamellar) and, usually at lower surfactant concentrations, various disordered analogues. Depending on surfactant geometry, salinity etc, there may be a preference for two-dimensional (sheet-like) or one-dimensional (worm-like) assemblies. In the latter case, one can envisage an ordered hexagonal or square arrangement of infinite cylinders, stable at high surfactant volume fractions ϕ, which will melt as the concentration is reduced and/or the temperature raised. The isotropic disordered phase which results should consist of an entangled mass of flexible worm-like objects, whose equilibrium statistics and dynamics resemble those of a polymer solution. From the opposite end of the concentration scale, one can envisage a system of small spherical micelles at low concentration, that undergo uniaxial growth to make rod micelles as the volume fraction of amphiphile is increased (in accordance with mass–action principles). At some length scale, the persistence length, these rods become flexible and behave as polymers. If the scission energy of a micelle (the energy required to create two end-caps from a semi-infinite cylinder) is large enough, then the semi-flexible linear micelles may become very long, and entangled with one another, at relatively low total volume fractions of surfactant (see figure 1).

There is now very strong evidence for an entangled micellar phase in several aqueous cationic detergent systems in the presence of added salt [1–21]. These include cetyltrimethylammonium bromide or chloride (CTAB or CTAC) with added KBr or sodium salicylate (NaSal); cetylpyridinium bromide (CPyBr) + KBr; cetylpyridinium salicylate (CPySal) + NaSal, etc. More recently similar effects have been seen in a reverse microemulsion system involving lecithin + trace water in isotane [22, 23].
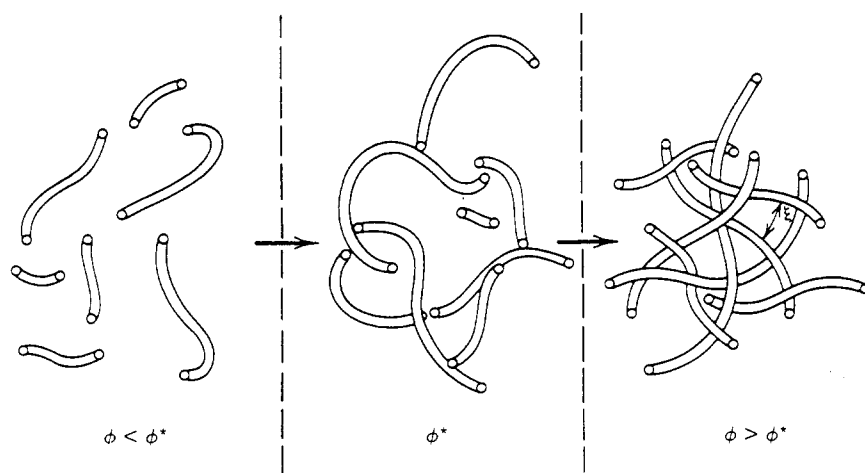
$\phi < \phi^*$ ϕ^* $\phi > \phi^*$

Figure 1. Schematic representation of the state of the solution with increasing surfactant volume fraction.

This list is not exhaustive: since the local stability of the semi-flexible cylinder is determined largely by packing considerations [24], we may expect to find worm-like viscoelastic phases in many homologous series of surfactants for appropriately chosen values of (say) the length of the hydrophobic tail. This should include anionic and non-ionic surfactants as well as the cationic species mentioned above.

In the rest of this article, we outline some progress that has recently been made in understanding the statistical physics of these systems. In section 2 we summarise theoretical predictions for the equilibrium statistics; in section 3 these are compared with experiments. sections 4 and 5 concern respectively theory and experiment for dynamical properties. Section 6 is a brief conclusion and summary of open issues.

2. Equilibrium properties: theory

Here we discuss the equilibrium statistics of locally cylindrical linear surfactant assemblies. At very low concentrations these systems show the normal properties of amphiphilic solutions with a critical micelle concentration (CMC) of the order of 10^{-4} for CTAB/KBr. Above the CMC, one expects the micelles to become larger due to the usual mass–action effects. For amphiphiles with a preference for spherical packing this growth is limited since a large spherical micelle cannot be made without a hole in the middle. If there is preference for cylindrical packing, there is in contrast the possibility of almost unlimited uniaxial micellar growth [24–28]. This we shall treat using the language of polymers. Our description is only valid for worm-like assemblies that are much longer than their persistence length l_p; as described below, experiments suggest that l_p is for CTAB/KBr of order 150 Å and the criterion is well satisfied at concentrations of a few per cent or more. The value of l_p is related to the rigidity modulus of the cylinder [25] which is in turn expected to depend quite strongly on the choice of surfactant and counterion, the salt concentration, etc. In fact, the Flory–Huggins theory presented in section 2.1 coincides in the low concentration limit to the laws of mass action appropriate to a system of *inflexible* micellar rods. It therefore provides a starting point for describing the system at any concentration far above CMC.

For cylinders that are long compared to l_p, the main departure from conventional theory of polymer solutions [29,30] is that in micellar systems, the reversibility of the self-assembly process ensures that (in polymer language) the *molecular weight distribution* (MWD) of the worm-like polymeric species is in thermal equilibrium. This contrasts with ordinary polymer solutions for which the MWD is fixed (quenched) and equilibrium only applies to the remaining (configurational) degrees of freedom. Systems where the MWD is free to vary are referred to as 'equilibrium polymers'. Apart from surfactant assemblies, there are several other occurrences of equilibrium polymers in nature, including poly-α-methylstyrene [31], plastic sulphur [32,33] and liquid selenium [34].

2.1. Mean-field theory

Whereas the MWD in an equilibrium polymer system is not fixed *a priori*, it can in principle be calculated using statistical mechanics. We start at the level of a Flory–Huggins [29] or mean-field approach [26,35]. We choose units so that $k_B T = 1$, and assume that no closed rings are present [36,37]. For a system of linear chains, inscribed for convenience on a unit lattice, the free energy may then be written as

$$F = \sum_L c(L)[\log c(L) + E] + (1 - \phi)\log(1 - \phi) \qquad (2.1)$$

where the number density of chains of length L is denoted by $c(L)$; E is the scission energy of the chain (as required to create two new chain ends) and we have defined the total volume fraction

$$\phi = \sum_L L\, c(L). \qquad (2.2)$$

In the first term of (2.1) we have, without loss of generality, set equal to zero the part of the free energy per chain that is extensive in chain length; since the term in ϕ also is extensive (it depends only on the total concentration) we may absorb this term, too, leaving finally

$$F = \sum_L c(L)[\log c(L) + E]. \qquad (2.3)$$

Minimizing with respect to $c(L)$ (paying attention to the constraint of (2.2)) yields

$$c(L) \propto \exp[-L/\bar{L}] \qquad (2.4a)$$

$$\bar{L} \simeq \phi^{1/2}\exp(E/2k_B T) \qquad (2.4b)$$

where the dependence on $k_B T$ has been restored. This is a classical result [24,26,27,35,36]. As noted above, equations (2.4) are also appropriate to the description of dilute, inflexible micellar rods, for which they reduce to the results of a mass–action calculation.

The above calculation is for an athermal solution of equilibrium polymers with a persistence length of unity. The addition of a mean-field interaction term $\propto \phi^2$ to (2.1) has no effect on $c(L)$ (unless a phase separation occurs); indeed, one may add to (2.1) an arbitrary function of ϕ without changing the outcome. Our choice of a unit lattice

is for convenience and amounts to using the persistence length l_p as the unit of length. (This choice influences the prefactors in (2.4); however, we ignore these prefactors for simplicity in what follows.) Another tacit assumption is that the scission energy E is local and independent of ϕ. This assumption may fail for highly charged micelles at low ambient salt concentrations, leading to a stronger dependence of $\bar{L}$ on ϕ than given in (2.4b) [38].

The Flory–Huggins approach regards each polymer as a free random walk that is uncorrelated with itself and with its neighbours. If the persistence length l_p is known, the results given above allow one to calculate the average gyration and hydrodynamic radii of the chains in terms of l_p, E and ϕ. The entire treatment ignores correlations brought about by the mutual avoidance of the chains; such correlations are normally dealt with using a scaling approach (see below). When the excluded volume repulsion of the chains is strong, the correlations are important in the dilute limit, and also in the 'semi-dilute' regime in which the chains overlap ($\phi \geq \phi^*$, the overlap threshold) while the total volume fraction of polymerised material is still small ($\phi \ll 1$). At higher concentrations, or for weak repulsions, the mean-field results derived above are appropriate. Apart from the presence of a variable mean chain length and strong polydispersity (2.4), the mean-field predictions for thermodynamic quantities coincide with those for ordinary polymer solutions. For example [29, 30], the free energy density is proportional to ϕ^2.

2.2. Scaling theory

It is simple to extend the above analysis to the case of a semi-dilute solution of chains, again assuming that no rings are present [35, 36]. This assumption is not always justifiable [37] but the calculation is nonetheless instructive. In semi-dilute solution we know that a mean-field approach remains valid so long as the basic 'monomer' is replaced by a 'blob' [29] of size

$$\xi \sim \phi^{\nu/(1-\nu d)} \sim \phi^{-0.77} . \tag{2.5}$$

Here d is the dimension of space, and ν is the swollen chain exponent $\simeq 0.588$. Thus we may write (again omitting an osmotic term that depends only on the overall concentration, ϕ)

$$F = \sum_L c(L)[\log c'(L) + E']. \tag{2.6}$$

In this expression

$$c'(L) = c(L)\xi^d \tag{2.7}$$

denotes the number density of L-chains measured in coarse-grained 'blob' units, and

$$E' = E - (d + \theta)\log\xi \tag{2.8}$$

where $\theta = (\gamma - 1)/\nu \simeq 0.3$. In (2.8), the first term is, as before, the scission energy of a bond. The second is more subtle: it is the free energy change resulting from the *gain in entropy* when a chain breaks so that the two new ends can explore a volume ξ. This entropy gain is enhanced by the fact that the excluded volume repulsion on scales less than ξ is also reduced by breaking the chain; this effect is accounted for by the term θ in the prefactor of $\log\xi$.

Now minimising (2.6) at fixed ϕ gives

$$c(L) \propto \exp(-L/\bar{L}) \tag{2.9a}$$

$$\bar{L} \simeq \exp(E/2k_{\mathrm{B}}T\,\phi^{y}) \tag{2.9b}$$

$$y = \tfrac{1}{2}[1 + (\gamma - 1)/(\nu d - 1)] \simeq 0.6. \tag{2.9c}$$

Thus the concentration dependence of the mean molecular weight $\bar{L}$ is described by an exponent y that differs slightly from the one predicted by simple mean-field theory ($y = \tfrac{1}{2}$, (2.4b)). As in the Flory–Huggins limit, thermodynamic properties such as the free energy density in the semi-dilute regime are unaffected by the fact that the MWD is in equilibrium; these properties depend only on the blob size ξ and not on how material is partitioned among chains of different lengths. Thus, for example, the free energy density (and with it the high frequency shear modulus) scales like $k_{\mathrm{B}}T\xi^{-d} \sim \phi^{2.3}$ as for normal semi-dilute polymer solutions [29].

For dilute solutions ($\phi \ll \phi^{*}$), the difference between the scaling results and those of Flory–Huggins theory are more marked. However, the main experimental data that we shall review below involves either the very dilute regime where the cylindrical micelles are relatively short (only a few persistence lengths) or the entangled, semi-dilute regime. To obtain very long flexible chains (that could show fully-developed excluded volume correlations) in dilute solution one requires a very high scission energy E (which leads to a very small ϕ^{*}). There is some evidence that this occurs in the system CTAC/NaSal, which has a ϕ^{*} value of order 10^{-3} M compared to typical values of 5×10^{-2} for CTAB/KBr.

2.3. Effects of rings

Although rings were ignored above, these should in principle lead to some changes to the scaling [36]. For the true semi-dilute limit (which, as the limit of zero concentration for infinitely long chains, requires $E \to \infty$) there are few large rings, but in principle one should expect the simple scaling picture (a mesh of blobs) to be 'decorated' with a cascade of rings on a scale smaller than the mesh size ξ. Petschek *et al* [36] have given a detailed treatment of these rather complicated effects which include (remarkably) a small decrease in the exponent ν. However, the rings may be suppressed in micellar systems for two obvious reasons: (i) the micelles may have a relatively long persistence length l_{p} relative to their diameter (this inhibits closure, at least for small rings); (ii) the micelles may have a not-too-large scission energy E (which would push the overlap threshold ϕ^{*} to relatively high concentrations). However, in either case one might expect excluded volume effects to be weakened, and hence to see mean-field exponents rather than those for scaling without rings [39].

On the other hand, a full off-lattice estimation of the ring-closure probability for micelles is quite complicated [37], and it is arguable that ring closure can be suppressed, without weakening of excluded volume, when the micellar diameter (as well as its persistence length) is large compared with a solvent molecule. In this case, the predictions coincide essentially with those of section 2.2 (scaling without rings) except at very low volume fractions. Since in any case the calculations with rings present are extremely complex, from now we consider only that version of the scaling theory and, for comparison, the Flory–Huggins theory of section 2.1.

3. Equilibrium properties: experiments

3.1. Dilute solution: effect of surfactant concentration

In dilute solution, the micellar size distribution can be probed by studying the scattering and hydrodynamic properties of the system [40]. Early estimates from light scattering experiments of the average molecular weight $M_{\rm W} \sim \bar{L}$ of the micelles, indicated a considerable increase of the aggregation number in some cases: up to 10^4 for instance for dilute CTAB in NaBr aqueous solutions [41]. The major problem encountered in an accurate determination of micellar molecular weight arises from the effect of the interactions which cannot be neglected for ionic surfactants (even at high dilution) and which strongly depends on the salt content. In 'ordinary' polymers this difficulty is overcome by extrapolating the experimental data to zero concentration. This procedure cannot be applied to the case of micellar solutions since the molecular weight of the micelles is an increasing function of the surfactant concentration ϕ. Despite these difficulties, several light scattering studies have been performed in very dilute systems where the micelles adopt a shape of small rigid rod. Measurements by Benedek *et al* [42–46] of the mean hydrodynamic radius and of the radius of gyration $R_{\rm G}$ of sodium dodecyl sulphate (SDS) micelles in 0.6 M and 0.8 M NaCl aqueous solutions in the SDS concentration range $2 \times 10^{-5}\,{\rm M}$–$10^{-3}\,{\rm M}$ provided results consistent with the $\phi^{1/2}$ dependence of the average aggregation number given in $(2.4b)$. (Recall that this result applies for dilute rods as well as for polymers.) Furthermore, the values obtained for the variance of the autocorrelation function of the scattered light indicated a rather large polydispersity, in agreement with the theory of section 2.1.

3.2. Effect of temperature

The temperature dependence of the averaged hydrodynamic and gyration radii $R_{\rm H}$ and $R_{\rm G}$ have been measured for the same SDS solutions. Both $R_{\rm H}$ and $R_{\rm G}$ are found to increase markedly as the temperature is reduced. This is consistent with the T dependence in $(2.4b)$. From the values obtained, assuming for the micelles a prolate ellipsoidal shape, the average length of the micelle has been determined. The fit of the exponential law of $(2.4b)$ to the experimental results yields the following value of the scission energy at room temperature: $E \simeq 20k_{\rm B}T$ at 0.8 M NaCl and $E \simeq 15k_{\rm B}T$ at 0.6 M NaCl [44–46].

Similar experiments were performed by Porte *et al* [1–4] on micellar systems under conditions where the micelles are longer than $l_{\rm p}$ and thus adopt a worm-like shape. Here the interpretation of the results is more complicated as it requires a model to relate $M_{\rm W}$ to $R_{\rm G}$ and $R_{\rm H}$. The scission energies obtained by assuming a flexible polymer model as suggested in section 2.1, are of the same order of magnitude as for the SDS systems described above. These results are in reasonable agreement with arguments based on geometrical packing criteria and/or a continuum elastic theory [25], which predict contributions to the micellar scission energy of roughly $k_{\rm B}T$ for each molecule that inhabits an end-cap region rather than the normal cylindrical environment.

3.3. Effect of added salt

The micellar growth is very sensitive to the nature and the amount of added salt. Figure 2 represents the variations of the hydrodynamic radius $R_{\rm H}$ of cetylpyridinium

salt micelles with the concentration of added salts (NaBr, NaCl) at fixed temperature (T = 35 °C) and surfactant concentration (6 × 10^{-3} M). It is seen that while NaBr is able to promote a large increase in micellar size (up to R_H = 650 Å), NaCl has no noticeable effect on R_H, which remains equal to 30 Å over a wide range of its concentration (0.1 M, 0.8 M). Only at higher salt concentration ($\sim$ 1 M) do the micelles start to grow. These findings suggest that the scission energy E is very strongly dependent on counterion-specific effects, a result found also for many other systems. This is quite reasonable when one considers that the counterions that remain bound to the surfactant molecules in a micelle may strongly perturb the local packing geometry.
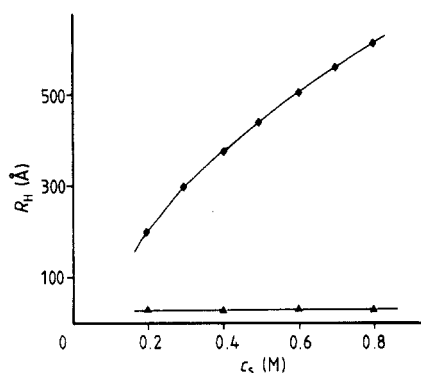

Figure 2. Hydrodynamic radius of cetylpyridinium bromide micelles as a function of salt concentration c_s : ($\Diamond$) NaBr; ($\triangle$) NaCl; T = 35 °C; concentration of cetyl pyridinium salt = 6 × 10^{-3} M. From [1].

3.4. Micellar flexibility

Static scattering techniques are usually well suited to determining the morphology of particles suspended in a fluid. Starting with the experimental scattered intensity $I(K)$ obtained from small angle neutron or x-ray scattering at wavevector transfer K, the usual method of analysis for the dilute regime is to fit the data to theoretical predictions for different particle shapes (rod, disk, flexible cylinder, etc) on the assumption that interactions among the particles may be neglected. Few attempts have been made to perform such fits for large flexible micelles [5]. The usual procedure is then to compare measurements of the radius of gyration found in this way with the hydrodynamic radius measured by quasi-elastic light scattering (QELS) at a finite concentration [2, 10, 42–47]. However, the wide polydispersity predicted theoretically, and confirmed experimentally by other techniques [6–9], make the data for worm-like micellar systems rather ambiguous.

The first unambiguous evidence of micellar flexibility was given by Porte *et al* in a study combining QELS and magnetic birefringence experiments on a CPyBr system [1]. In QELS, one measures the temporal autocorrelation function of the scattered light intensity, thus obtaining information about the mean hydrodynamic radius (i.e. the reciprocal of the diffusion constant) of the particles, and its variance. The QELS results are summarised in figure 2; as discussed in the previous section, they show that CPyBr micelles undergo a large growth upon increasing NaBr concentration, whereas there is no corresponding increase in R_H size upon addition of NaCl.

In the magnetic birefringence technique one measures the Cotton–Mouton constant $C_{CM} = \Delta n/H^2$, where Δn is the optical birefringence and H the applied magnetic field. Figure 3 shows the variation of C_{CM} with salt concentration for aqueous CPyBr. No variation is observed when NaCl is the added salt, which corroborates the behaviour of R_H just described. On the other hand, when NaBr is the added salt, one observes in the low NaBr concentration range an increase of C_{CM}, followed by a plateau for [NaBr]≥ 0.2 M which corresponds to a hydrodynamic radius $R_H \simeq 200$ Å. The initial increase of C_{CM} was interpreted as a micellar growth, the micelles adopting a rigid-rod shape. The stiff cylindrical micelles reorient in the magnetic field to produce an optical response with C_{CM} proportional to the length of the micelles. At higher NaBr concentrations, the Cotton–Mouton constant reaches a saturation value, while the R_H variations still indicates a steady growth with further added salt. These results are consistent with a worm-like micellar structure, characterised by a persistence length l_p, defined as the length over which the cylindrical micelle can be considered as rigid. Parts of any given micelle, separated by contour length much larger than l_p, align independently in the magnetic field roughly as if they were unconnected small rods of length l_p. A more detailed analysis of the results shown in figures 2 and 3, allowed Porte *et al* to obtain a quantitative estimate of the persistence length as $l_p \simeq 200$ Å.
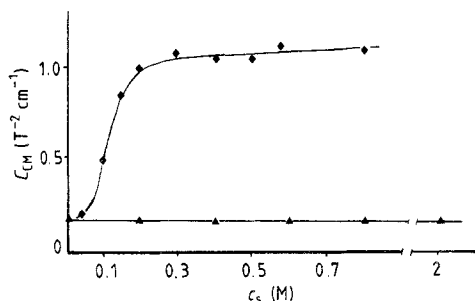

Figure 3. Cotton–Mouton constant of cetylpyridinium bromide micellar solutions as a function of salt concentration c_s : (◊) NaBr; (△) NaCl; $T = 35$ °C; concentration of cetyl pyridinium salt $= 6 \times 10^{-3}$ M. From [1].

Several small angle neutron scattering (SANS) studies have been carried out to probe the local structure of large micelles, mainly by the Bayreuth group [15–17, 48–50]. All studies but one [48] have inferred a unidimensional growth of the micelles upon increasing the surfactant or/and salt concentration; most of the data was fit using a stiff micelle model. Very recently, Porte [51] was able confirm by SANS the persistence length estimated by QELS and magnetic birefringence for CPyBr in 0.8 M NaBr solutions. The surfactant concentration was 6×10^{-3} M and the temperature $T = 35$ °C. The form factor was determined over a very wide K range (3×10^{-4} Å^{-1}– 0.4 Å^{-1}) by combining light scattering and SANS data; analysis based on the hypothesis of a worm-like object provided the following micellar parameters:

$$R_G = (740 \pm 50)\,\text{Å} \qquad l_p = (160 \pm 30)\,\text{Å} \qquad r_c = (20 \pm 1)\,\text{Å}$$

where r_c is the radius of the cylinder (the value quoted being consistent with the

length of the surfactant molecule). The agreement between the value of l_p and that of the previous finding (200 Å) is excellent.

3.5. Crossover to the semi-dilute regime

QELS provides a convenient method to probe the crossover between the dilute and semi-dilute regimes for worm-like micellar solutions. In the dilute range the measurement of the autocorrelation function of scattered light allows one to determine the translational diffusion coefficient of the micelles as described above. The micellar growth associated with the increase of surfactant concentration should produce a decrease of the diffusivity of the particles up to the concentration ϕ^* where the thread-like micelles begin to overlap. Beyond this concentration the time dependence of the concentration fluctuations is described by a cooperative diffusion mechanism [29]. As with ordinary polymer solutions, the corresponding collective diffusion constant D is independent of the lengths of the micelles, since the average micelle is large compared to the mesh-size ξ. D is related to the hydrodynamic correlation length ξ_H through

$$D = k_B T / 6\pi\eta_s \xi_H \qquad (3.1)$$

As ξ_H scales like ξ (cf. (2.5)) then D should *increase* with surfactant concentration in the semi-dilute regime. Therefore the diffusion constant measured experimentally from the correlation function of scattered light should exhibit a minimum at the overlap concentration ϕ^*.

Such a behaviour is illustrated by figure 4 which shows the concentration dependence of the collective diffusion coefficient at several temperatures, for aqueous solutions of a system containing cetyltrimethyl ammonium chloride (CTAC) and sodium salicylate (NaSal) at fixed molar ratio in the presence of 0.1 M NaCl. The data have been corrected for the change of solvent viscosity η_s with temperature, and are plotted as $\log(D\eta_T/\eta_{25\,^\circ C})$ versus $\log C$, where η_T denotes the solvent viscosity at temperature T. The results in the dilute range show clearly the increase of micellar size upon increasing surfactant concentration or decreasing temperature. The latter effect causes the shift of the minimum towards lower concentrations, as the crossover concentration ϕ^* is expected to decrease as the micellar size increases. In the semi-dilute range, the corrected diffusion constant $D\eta_T/\eta_{25\,^\circ C}$ is almost temperature independent in agreement with a polymer-like model for which the correlation length ξ, or equivalently ξ_H, does not depend on the sizes of individual chains but only on the overall volume fraction of the polymer. (More exactly, this predicts for the corrected diffusion constant a linear dependence on absolute temperature which would be barely detectable on the plot shown.)

The crossover between dilute and semi-dilute regimes can also be seen in measurements of the intensity of scattered light. At high dilution this increases with concentration, reflecting the increase of the micellar molecular weight, whereas at high volume fraction it decreases, reflecting the decrease of the osmotic compressibility. Evidence of such behaviour (maximum of scattered intensity and minimum of diffusion coefficient) can be observed in the data of several authors [42, 10, 6-8, 18].

3.6. Semi-dilute scaling behaviour with surfactant concentration

The scaling behaviour of the correlation length ξ as a function of surfactant concentration, (2.5), can be tested experimentally through different physical quantities.
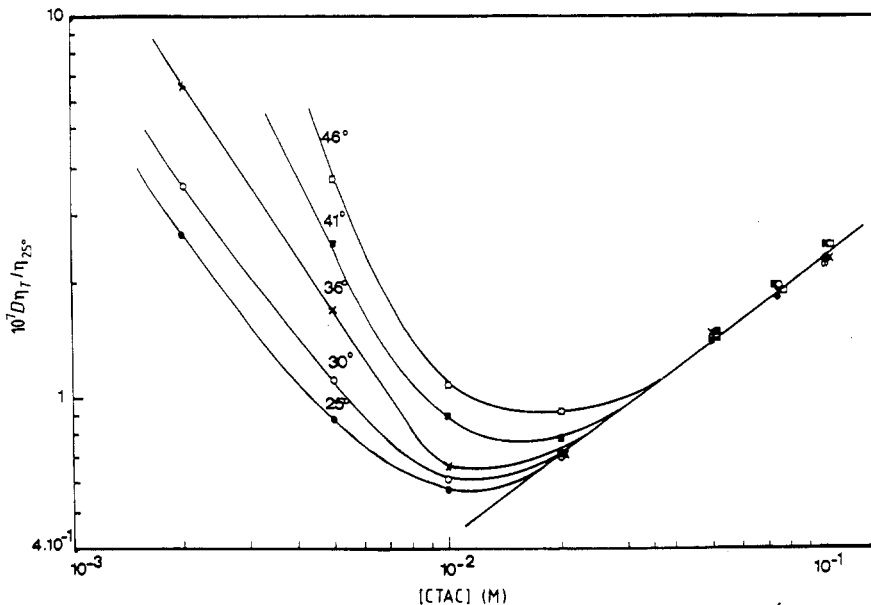
Figure 4. Variation of the diffusion coefficient corrected for viscosity, $D\eta_T/\eta_{25^\circ C}$, as a function of the surfactant concentration and at different temperatures, as indicated on the plots. The straight line through the points at high concentration has a slope 0.77. From [8].

In principle, a direct determination of ξ can be obtained from scattering measurements in the semi-dilute range. So far, the only data are for light scattering [18]; although results have obtained in a rather limited concentration range, these are reasonably well-fit by the scaling prediction (without rings) for strong excluded volume, i.e. $\xi \sim \phi^{-0.77}$.

The concentration dependence of ξ can also be inferred from that of D. The data of figure 3 are best fitted in the semi-dilute range with a straight line of slope 0.73. Results obtained in a large variety of systems show the general features illustrated by figure 3 but the exponent of the power law of D versus ϕ was found to vary between 0.6 and 0.8 [6–8,52,11,53]. In this respect one must remark that similar deviations from the limiting behaviour described by (2.5) have been observed for polymer solutions when either the molecular weight of the polymer was not large enough, or the solvent was insufficiently good (marginal) [54]. In this case one expects $\xi \sim \phi^{-1/2}$ as predicted from a mean-field approach.

The most accurate determination of the exponent of the power law of $\xi(\phi)$ is probably through the measurements of the shear modulus G_0 which for semi-dilute polymers is related to ξ by

$$G_0 \simeq k_B T/\xi^3 \qquad (3.2)$$

Figure 5 represents the variations of G_0 for the same systems as in figure 3 [55]. The data are well fitted by a straight line with a slope close to the theoretical one. This result has also been obtained for several other systems [56,57]. It is also found that the shear modulus is only weakly dependent on temperature, which corroborates the results obtained for the diffusion coefficient.
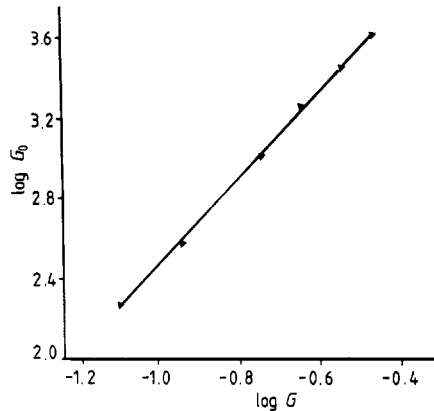
Figure 5. Variation of the shear modulus as a function of surfactant concentration for the system CTAC/NaCl (1/0.6)/0.1 M NaCl. The data correspond to averaged values in the range 30 °C to 50 °C. From [55].

It should be emphasised that, due to uncertainties about the strength of the excluded volume interaction (which may be weak when the persistence length is relatively long compared to the cylinder diameter), the theoretical justification for these scaling laws for worm-like micelles is less clear than for conventional semi-dilute polymers. In particular, it would not be surprising to find that for many systems the behaviour is closer to mean field than to semi-dilute scaling (even at relatively low concentrations). We should also note that for ionic surfactants at low added salt, and low ϕ, polyelectrolyte effects become important, leading to behaviour that cannot be explained within the framework outlined above.

4. Dynamical properties in the entangled state: theory

In this section we consider dynamical properties such as self diffusion (as opposed to the collective diffusion phenomena discussed above) and viscoelasticity. We focus on the entangled regime ($\phi \gg \phi^*$) although some of our arguments have parallels for dilute systems. Throughout this section we presume that the micelles are much longer than the persistence length l_p. We start by outlining the dynamics of entangled, unbreakable polymers of a single chain length, which are understood in terms of the reptation model [30]. Subsequently we modify this approach to allow for reversible chain breakage processes, which are found to substantially alter the self-diffusion and viscoelastic relaxation spectra.

4.1. The reptation model for unbreakable chains

The dynamics of entangled, unbreakable polymers are quite well understood in terms of the reptation model [30, 29]. In this model, relaxation of chain conformations occur by the gradual disengagement of any given chain, by curvilinear diffusion along its own contour, from a tube-like environment. The tube consists of neighbouring chains; these present a set of obstacles to diffusion normal to the chain contour.

If a small strain is applied to the system at time zero, a stress is induced, which is associated with the entropy loss of the polymer chains on deformation. As each

chain reptates out of its original tube, new tube is created that is in equilibrium in the strained environment, and so carries no stress. Thus the fraction of stress, $\mu(t)$, remaining at time t is just the fraction of the original ($t = 0$) tube that is still occupied at time t (i.e. through which neither end of the chain has passed). For a monodisperse system in which all chains have the same length, $\mu(t)$ is easily computed [30] as

$$\mu(t) = (8/\pi^2) \sum_{p=\text{odd}} p^{-2} \exp(-tp^2/\tau_{\text{rep}}) \tag{4.1}$$

which is a nearly pure exponential decay, with longest relaxation time

$$\tau_{\text{rep}} \simeq \overline{L}^2/D_{\text{c}} . \tag{4.2}$$

Here $D_{\text{c}}(L) \sim 1/L$ denotes the curvilinear diffusion constant of the chain in its tube. The corresponding real-space diffusion constant of the chain obeys $D_{\text{rep}}\tau_{\text{rep}} \simeq R_{\text{G}}^2$ with R_{G} the gyration radius. An object of interest is the stress relaxation function $G(t) \equiv G_0\mu(t)$ where G_0 counts the number of entropic degrees of freedom effectively coupled to the strain. This quantity, the plateau modulus, is found to vary with polymer density ϕ as

$$G_0 \sim \phi^a \tag{4.3}$$

$$a \simeq 2.3 \pm 0.2 \tag{4.4}$$

for most polymeric systems. This is consistent with the semi-dilute scaling law, (3.2), but appears empirically to be valid also in relatively dense systems.

The viscosity of the system obeys $\eta = \int_0^\infty G(t)\,dt$; all other linear viscoelastic functions may also be derived if $G(t)$ is known.

4.2. Role of reversible scission reactions

We next consider how these results are modified in the presence of a dynamic equilibrium involving rupture and recombination of the chains. The first effect, of course, is to enforce equilibrium of the MWD as described by (2.4) or (2.9). If the reaction kinetics are exceedingly slow, so that negligible breaking occurs on the time scale of disengangement of a typical chain (of length $\overline{L}$), then this is the *only* effect. At a first approximation [58], we can construct the relaxation function $\mu(t)$ as the weighted average of (4.1) over the chain length distribution $c(L)$ (2.2). At the level of steepest descents one finds

$$\mu(t) \sim \exp[-\text{constant} \times (t/\tau_{\text{rep}})^{1/4}] \tag{4.5}$$

where here and below, τ_{rep} denotes $\tau_{\text{rep}}(\overline{L})$ obeying (4.2). This represents an extremely non-exponential decay of stress; a similar effect is predicted for the self-diffusion relaxation spectrum.

Experimentally, as described in the next section, for several of the entangled worm-like surfactant systems mentioned in section 1, an extremely pure exponential stress-decay curve is seen [19–21, 13]. (A single relaxation time is also seen in the self-diffusion measurements [9].) This demonstrates that the kinetics whereby micelles break and reform, is fast enough to directly affect the stress relaxation process [19]. To understand this new regime it has been found helpful to introduce a specific model

[58] for the scission and recombination reactions (although many of the qualitative conclusions are more general). In this model we assume:

(i) scission of a chain is a unimolecular process, which occurs with equal probability per unit time per unit length on all chains. The rate of this reaction is a constant k for each chemical bond; more usefully one can introduce the parameter

$$\tau_{break} = 1/(k\bar{L}) \tag{4.6}$$

which is the lifetime of a chain of the mean length $(\bar{L})$ before breaking into two pieces;

(ii) recombination occurs as a bimolecular process, with a rate that is independent of the molecular weights of the two reacting subchains; moreover there are sufficient ends in the system that a chain is unlikely to recombine with its partner from the preceding dissociation (a mean-field assumption). It is then easily shown, by detailed balance, that the lifetime of a free chain end before recombination is also τ_{break}.

These assumptions are restrictive, but interesting since they allow the coupled reaction/reptation equations to be cast as a one-dimensional stochastic process whose statistics can be worked out numerically [58]. It is found that if the breaking time is long ($\tau_{break} \gg \tau_{rep}$) the stress relaxation function $\mu(t)$ indeed obeys (4.1) as expected. However, for smaller τ_{break}, $\mu(t)$ becomes more like a single exponential (see figure 6); when $\tau_{break} \ll \tau_{rep}$ a clean single exponential is seen with decay time

$$\tau \simeq (\tau_{break}\tau_{rep})^{1/2}. \tag{4.7}$$

This value for the terminal time may be explained by observing that the time taken for the stress associated with a typical tube segment to relax is the waiting time for a chain end to pass through that segment. Such a chain end has a finite lifetime τ_{break}, during which it can move by reptation a curvilinear distance l obeying roughly $D_c(\bar{L})l^2 \simeq \tau_{break}$. For this end to pass through the given tube segment within its lifetime, it must originate from a break in the chain within a distance $\simeq l$ from that tube segment, measured along the tube. The rate limiting step consists of waiting for this initial break to occur; this takes a time $\tau \simeq 1/(kl) \sim (\tau_{break}\tau_{rep})^{1/2}$. Similar arguments [58] applied to the diffusion constant yield $D \sim D_{rep}(\tau_{break}/\tau_{rep})^{-1/3}$. These results apply so long as the lifetime of a chain end is long enough that it moves predominantly by curvilinear diffusion, rather than by a more local dynamics which is relevant at shorter time scales [30]. Crossovers to several further regimes at small τ_{break} heve been described [58]; in these regimes the dependence of τ on τ_{break} and τ_{rep} is modified, whereas the mono-exponential behaviour should remain.

The single exponential stress decay can be explained by noting that the relaxation mechanism, described above, involves all tube segments equally. Before a given tube segment relaxes (in time $\tau \gg \tau_{break}$) the chain occupying it typically undergoes many scission and recombination reactions, so that there is no memory of either the initial length of the chain, or the position on the chain initially corresponding to that tube segment. Thus all tube segments relax at the same rate; there is no dispersion of relaxation times. Similarly there is no dispersion in the self-diffusion spectrum. In section 4 we shall see that a single exponential stress relaxation is a characteristic experimental feature of many viscoelastic surfactant solutions.

The above results were found for a unimolecular scission model with uniform breaking. An alternative reaction involves 'end-interchange' whereby a free end attacks an interior bond of another chain. This bond breaks to form two new ends, one of which combines immediately with the attacking end, the other remaining free. If τ_{break} is
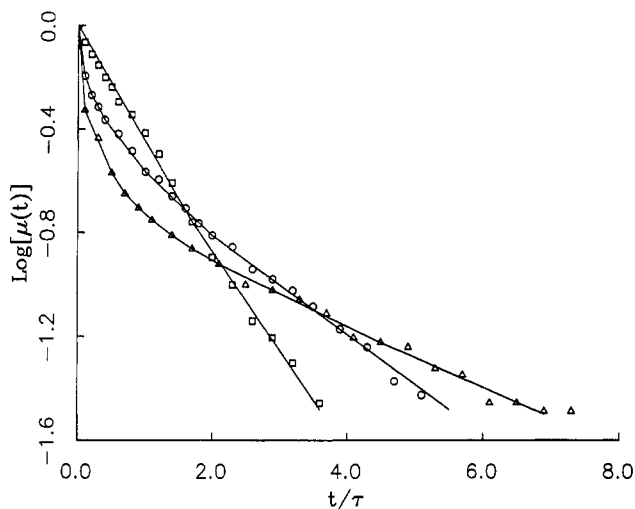
Figure 6. Log-linear plots of the stress relaxation function $\mu(t)$ against time for $\zeta = 0.01$ (squares) $\zeta = 2.75$ (circles) and $\zeta = 3100$ (triangles). Here $\zeta \equiv \tau_{\text{break}}/\tau_{\text{rep}}$. The time axis for each curve is scaled by the relaxation time $\tau = \int_0^\infty \mu(t)\mathrm{d}t$. Theoretical curves, from [58]. The solid curves are to guide the eye. Note that for small ζ the decay approaches single exponential (a straight line on this plot).

still defined as the lifetime of a chain before a reaction occurs somewhere along its length, then the previous analysis remains applicable (to within order unity factors). A third possible reaction involves bimolecular exchange of two interior bonds via a four-armed intermediate. In contrast to either of the previous reactions, this bond-interchange mechanism can lead to the relaxation of stress without the involvement of a chain end. The effect can be modelled using a transient network description [14] rather than a tube. However, experiments on other types of transient network do not usually lead to a single exponential relaxation time, and we see no reason why such behaviour should result from this mechanism. Since a single exponential decay is seen experimentally, we may hypothesise that this type of reaction does not play a major role in the systems studied so far. It is in any case a question of detailed chemistry which of the various possible reactions predominates in a given system. Other possibilities include reactions whereby surfactant molecules 'evaporate' singly or by the shedding of small micelles at the ends of a chain. The case when this predominates can be treated; it too does not lead to exponential decay.

4.3. Concentration dependence of the terminal time

The pure exponential decay seen in worm-like surfactant phases is consistent with the modified reptation model described above. Clearly one would like to use the model to explain the concentration dependence of the relaxation times [39]. The simplest model for the concentration dependence is to assume a spontaneous unimolecular scission rate that is independent of concentration. In this case one can calculate the ϕ-dependence of τ_{break}; one may also estimate τ_{rep} using a semi-empirical relation $\tau_{\text{rep}} \sim \bar{L}^3 \phi^2$ found for the case of unbreakable polymers in the mean-field regime [39]. Combining these according to (4.7) we obtain

$$\tau \sim \phi^b \qquad b \simeq 3/2 \tag{4.8}$$

and by similar arguments for the self-diffusion constant

$$D \sim \phi^{-c} \qquad c \simeq \tfrac{5}{3}. \tag{4.9}$$

The corresponding results of a scaling theory without rings (cf. section 2.2 above) are

$$b \simeq 1.4 \qquad c \simeq 1.7. \tag{4.10}$$

Further shifts in exponents are predicted for the case of end-interchange kinetics, and in the various further regimes that arise when the lifetime of a chain end is short enough that its motion is not by pure reptation, but involves fluctuation modes [58,33].

These predictions for the exponents b and c are based on the assumption of a ϕ-independent value of the scission energy, E. For ionic surfactant micelles, this assumption should be valid at high enough salt concentration, but may fail at lower salt levels [38].

4.4. Non-linear viscoelasticity

The above discussions are concerned solely with the regime of linear response theory, for which all viscoelastic functions are determined once $G(t)$ is known [30]. It is possible, under certain conditions, to extend the analysis to include non-linear viscoelastic effects. The assumptions are, (i) that the flow rate is high enough to cause significant non-linear deformations to the polymer configurations, but not so high as to directly perturb the chemical rate equations for scission and recombination; and (ii) that the stress is dominated by polymer entropy contributions rather than terms of non-polymeric origin. With these assumptions, the non-linear viscoelastic functions for equilibrium polymers (in the regime for which the linear response is single exponential stress decay) are predicted to be very similar to those found in the reptation theory of unbreakable, but *monodisperse* polymers, so long as the new expression (4.7) for the terminal time is taken into account [59,60]. Thus any strong departure from normal polymeric behaviour in non-linear flows (such as shear thinning, rod climbing, die-swell, etc) indicates a breakdown of one or other assumption made above. Strong departures are indeed seen in some systems [14,21] and theoretical work aimed at relaxing these assumptions is in progress [61].

5. Dynamical properties: experimental results

5.1. Dynamics of stress relaxation

The model described above predicts a stress relaxation spectrum that depends strongly on the parameter $\zeta = \tau_{\mathrm{break}}/\tau_{\mathrm{rep}}$; for $\zeta \ll 1$ the relaxation function $G(t)$ is almost single exponential whereas for $\zeta \gg 1$ it approaches a stretched exponential behaviour. The parameter is a strongly decreasing function of $\bar{L}$ since the breaking time decreases whereas the reptation time increases as the chains get longer. Indeed for the mean field regime one may estimate ζ as

$$\zeta \sim k^{-1} \bar{L}^{-4} \phi^{-2} . \tag{5.1}$$

Thus the micellar growth that is promoted by an increase in salt and/or surfactant concentration leads to a decrease in ζ and a narrowing of the relaxation spectrum, accompanied by an increase in the terminal relaxation time τ.
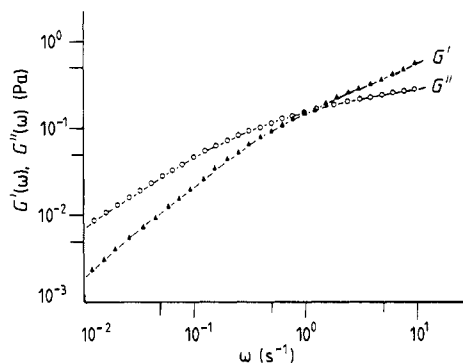
Figure 7. Storage modulus G' and loss modulus G'' as a function of the angular frequency ω for solutions of 1.5×10^{-2} M CPySal and 1.1×10^{-2} M NaSal at $T = 20\ ^\circ$C. From [21].
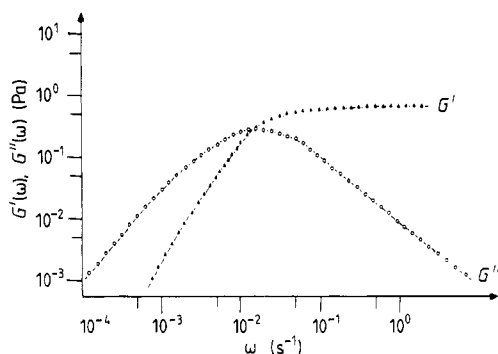
Figure 8. Storage modulus G' and loss modulus G'' as a function of the angular frequency ω for solutions of 1.5×10^{-2} M CPySal and 1.25×10^{-2} M NaSal at $T = 20\ ^\circ$C. From [21]. The dotted lines correspond to a fit to the Maxwell fluid (single-exponential $\mu(t)$).

This behaviour has been observed experimentally in several systems [19, 56, 21, 13]. It is illustrated in figures 7 and 8, which show the frequency dependence of $G'(\omega)$ and $G''(\omega)$, the real and imaginary parts of the dynamic shear modulus $G(\omega) \equiv i\omega \int_0^\infty \exp(-i\omega t)G(t)\mathrm{d}t$, for aqueous solutions of CPySal at two different salt concentrations. At the higher salt concentration (figure 8) the curves can be very well fit by a 'Maxwell fluid' or single exponential form for $G(t)$. This is particularly apparent when G' and G'' are plotted in a Cole–Cole representation [14], as shown in figure 9. At low salt concentrations, however, there is instead a disperse spectrum of relaxation times, as one would expect from a polydisperse system of effectively unbreakable chains (i.e. $\zeta \gg 1$). Similar results have been observed in aqueous CTAB/NaSal [14]. For aqueous CTAB solutions in excess KBr, a single exponential decay in the stress relaxation function has been observed over the whole concentration range investigated [56, 57], within the experimental accuracy of the magnetorheometer used for these experiments.

However, we remark that, in contrast to oscillatory devices, this apparatus does not have the accuracy required to see deviations from single exponential behaviour that are expected to occur in the short time range (i.e. the initial part of the decay curve.)
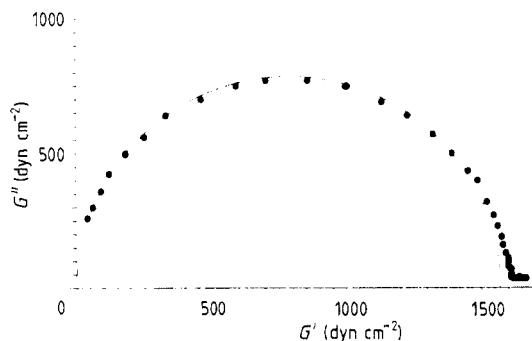

Figure 9. Cole–Cole plot of G' and G'' data for CTAC/Na Sal (1/0.6)/0.5 M NaCl; $T = 30°C$, $c = 0.2$ M. From [55].

5.2. Comparison with T-jump measurements

The nature of the relaxation mechanism can be elucidated further by comparing the decay times obtained from stress relaxation experiments and from temperature jump measurements. In the T-jump technique, a small step increase of temperature (0.1 to 1°C) is produced, generally by the discharge of a capacitor across the solution [40]. The resulting shift in the equilibrium of the system is usually monitored by a change in some optical property. For example, observation of the time dependence of the scattered light intensity provides kinetic information on the micellar breaking and recombination process. In particular, for the reversible scission reaction scheme with fixed rate constants k and k' (see section 4.2 above), it has been shown [62] that the chain length distribution decays after T-jump with a relaxation time $\tau_{break}/2$. Thus the scattered light intensity should also decay with this time constant.

The reptation model with scission, previously decribed, predicts single exponential relaxation for $\zeta = \tau_{break}/\tau_{rep} \ll 1$ which in turn implies that the chemical relaxation time τ_{break} is short compared to the terminal time for stress relaxation, $\tau = (\tau_{rep}\tau_{break})^{1/2}$. Measurements of τ_{break} from T-jump have been performed on CTAB/0.25 M KBr solutions and the results compared with those of τ for the same system [57,63]. As shown in figure 10, the breaking time decreases strongly with ϕ whereas the terminal time increases. In fact, the temperature dependence of the intensity is strongest in the dilute regime, becoming very weak in the highly entangled state whose thermodynamics are relatively insensitive to the MWD as discussed in section 2. This means that direct measurements of τ_{break} at high concentrations are impracticable; however, the extrapolated values of τ_{break} in this regime are equal to or smaller than the terminal time at each concentration. This is consistent with the observation of single exponential stress relaxation in this regime. T-jump and stress relaxation data for various viscoelastic surfactant systems have also been compared by the Bayreuth group [19,20], who report τ/τ_{break} of order unity (though generally
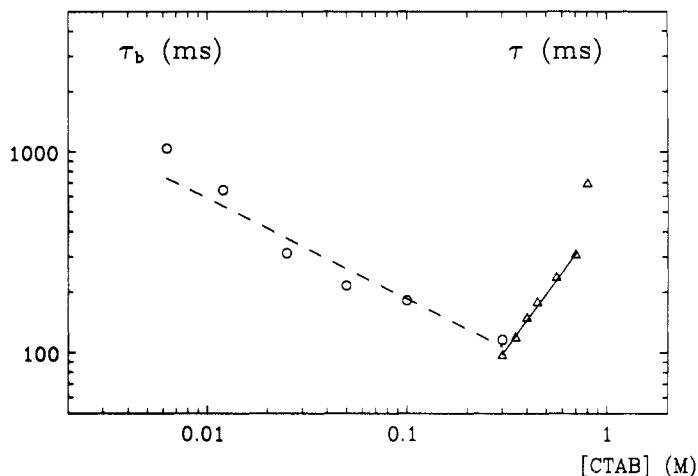
Figure 10. Variation of the breaking time τ_{break} and of the terminal time τ for stress relaxation as a function of CTAB concentration for 0.25 M KBr solutions at $T = 30\ ^\circ$C. The broken line has slope $-\frac{1}{2}$. From [63].

larger than one) for the samples studied which cover a relatively limited concentration range.

We believe that the explanation of a pure single exponential stress relaxation in the regime of $\tau_{break} \ll \tau_{rep}$ argues persuasively in favour of the model described in section 4.2. The prediction does not depend in detail on the reaction kinetics (so long as bond-interchange processes do not dominate); the origin of the narrow relaxation spectrum is in a rapid averaging (on the time scale τ_{break}) over factors such as chain length that would normally lead to a dispersion in the relaxation rates for different tube segments. The remaining experimental evidence discussed below, though largely consistent with the same model (at least for high salinities), is perhaps of secondary significance compared to the observation of single exponential decay — which is not found to similar precision in any other class of viscoelastic material known to us.

5.3. Effect of surfactant concentration

The system most thoroughly investigated, with a view to determination of scaling laws with volume fraction, remains aqueous CTAB in the presence of excess KBr. Log–log plots of the terminal time τ, the viscosity η and the self-diffusion constant D are shown in figures 10 and 11. The last of these is measured by the FRAP technique (flourescence recovery after photobleaching) [9], in which a periodic pattern is created in the sample by interference of two pulsed laser beams. Tagged molecules carrying a fluorescent group are activated by the incident light; when this is switched off there is a spatially periodic fluorescence signal which decays away under the influence of self-diffusion. (In the concentration range shown, this method reveals a single exponential spectrum, consistent with the modified reptation model and with the viscoelastic data.)

The variations of τ, η and D can be fit to power laws over concentration ranges covering about half a decade for τ and a decade or more for η and D. Although the concentration range covered is relatively small, there is some interest in comparing the 'exponents' with the theoretical predictions. The results are shown in table 1, where
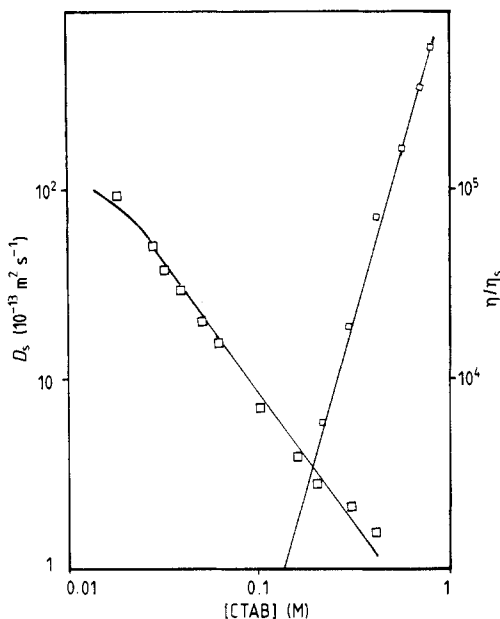
Figure 11. Variation of the reduced viscosity and of the self-diffusion coefficient as a function of CTAB concentration for 0.25 M KBr solutions at $T = 30\ ^{\circ}$C. From [57] and [9].

the three exponents are defined by $\tau \sim \phi^{\alpha_\tau}$, $\eta \sim \phi^{\alpha_\eta}$ and $D \sim \phi^{-\alpha_D}$. From section 4.3 we have $\alpha_\tau = b$ (4.8), $\alpha_\eta = a + b$ and $\alpha_d = c$ (4.9). Experimental values [55] for the system CTAC/NaSal (1/0.6)/0.1 M NaCl are also shown. The exponents are somewhat temperature dependent but are close to the theoretical predictions of the modified reptation model.

This agreement is, however, only attained at high added salt levels. The effects of salinity on the exponents have been investigated for CTAB/KBr systems [9,56,57]. It was found that a decrease in salt concentration below about 0.2 M produces a strong increase in each of the α exponents defined above. This is possibly associated with an electrostatic correction to the scission energy E which may lead to an explicit dependence of E on ϕ when the added salt level is small [38]. The correction to E is a decreasing function of concentration which leads to a stronger dependence of $\bar{L}$ (the average chain length) on ϕ than suggested by the theory presented in sections 2 and 4. Obviously, in view of this strong salt dependence, one would not wish to claim that the data summarised in the table confirm the model of section 4.2; however, they are broadly consistent with it.

The surfactant and salt concentration dependence of the stress relaxation time τ has also been studied for salicylate-containing systems [14], in which there appears to be evidence of specific 1:1 complexation with CTAB which leads to a highly non-trivial dependence of the decay time τ on the salt concentration and on ϕ. A similarly complex non-monotonic dependence of the relaxation time on added salt levels is found in the CPySal system [21]. To eliminate the complications associated with counterion effects, comprehensive experiments on non-aqueous systems could prove very useful. Very recently, a study has been made on a system of lecithin/organic solvent (+ trace water) [23], which appears to be a polymer-like phase as elucidated by neutron and

Table 1. Theoretical and experimental values of the exponents of the power laws as a function of surfactant concentration of η, T_R and D_s, for two systems

Temp. (°C)	Method	α_η	α_{T_R}	α_{D_s}
	Scaling†	3.7	1.4	−1.7
	Mean field†	3.5	1.5	−5/3
	Experimental values for CTAB–0.25 M KBr solutions [9, 57]			
24.6		3.45 ± 0.2	1.1 ± 0.15	
29.7		3.55 ± 0.2	1.25 ± 0.15	−1.4 ± 0.1
34.6		3.75 ± 0.2	1.3 ± 0.15	−1.57 ± 0.15
	Experimental values for CTAB/NaSal (1/0.6)–0.1 M NaCl solutions [55]			
30		3.27 ± 0.2	1.09 ± 0.15	
39.5		3.4 ± 0.2	1.23 ± 0.15	
49.6		3.52 ± 0.2	1.37 ± 0.15	

† Theoretical values.

dynamic light scattering techniques. Here, however, the viscosity exponent α_η appears to be anomalously low ($\simeq 1.9$) which suggests a terminal relaxation time that actually *decreases* with increasing concentration. This remains unexplained at present.

5.4. Effect of temperature

The temperature dependence of τ and of τ_{break} for the CTAB /KBr system are shown in figures 12 and 13 respectively. The linearity of the data when plotted as $\log(\tau/\eta_s)$ versus $1/T$ (with η_s the pure solvent viscosity and T the absolute temperature) indicates that both relaxation times follow Arrhenius laws of the form

$$\tau \sim \eta_s \exp[E_r/k_B T] \qquad (5.2a)$$

$$\tau_{\text{break}} \sim \exp[E_b/k_B T] \qquad (5.2b)$$

where we have defined effective activation energies E_r and E_b for the stress relaxation time τ and the breaking time τ_{break} respectively. The results obtained from the data of Figs. 12 and 13 are, in temperature units ($k_B = 1$),

$$E_r = 12\,700 \pm 1000 \qquad E_b = 14\,300 \pm 300 \,. \qquad (5.3)$$

Note that for normal (unbreakable) polymers, τ/η_s is a weak function of temperature, in complete contrast to these results for CTAB micelles. The strong dependence arises from the decrease in the average micellar length $\bar{L} \sim \exp(E/2k_B T)$ and the increase in the scission rate constant k on raising the temperature. T-jump experiments suggest that the activation energy E_A associated with the rate constant k is in fact rather larger than E, suggesting that a fairly high energy intermediate state is involved in the 'pinching apart' of two end-caps. Note that since $\tau_{\text{break}} = 1/k\bar{L}$, this E_A is related to E_b via $E_b = E_A - E/2$. Moreover, since $\tau_{\text{rep}} \sim \bar{L}^3$ (4.2) with a proportionality constant that depends only weakly on temperature (through the solvent viscosity), one has for the effective activation energy for stress relaxation

$$E_r = \tfrac{1}{2}(E_b + 3E/2) \,. \qquad (5.4)$$

This is a direct consequence of the result $\tau = \left(\tau_{\text{rep}}\tau_{\text{break}}\right)^{1/2}$, (4.7), for stress relaxation in the modified reptation regime. Inserting (for CTAB/KBr) the measured values of E_r and E_b in the above relationship yields $E \simeq 7000\,\text{K}$ in temperature units or $E \simeq 24k_B T$ at room temperature. This implies a scission energy that amounts to roughly $k_B T$ for each surfactant molecule that occupies an end-cap region rather than a fully cylindrical environment; this is close to what one would predict from packing arguments.
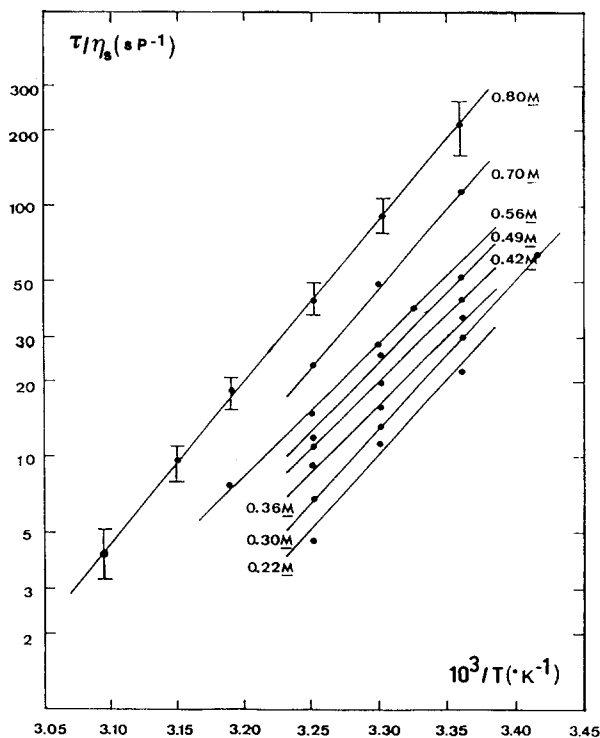

Figure 12. Variations of the terminal time τ for stress relaxation as a function of $10^3/T$ for CTAB–0.25 M KBr solutions.

In summary, for CTAB/KBr the temperature dependence of the T-jump and stress relaxation times appear to be consistent with the scission-modified reptation model in its simplest form. Similar work on other systems would be of interest; in particular, the relationship between the various effective activation energies depends on the type of reaction kinetics, and would be different for end interchange reactions, for example.

5.5. Non-linear viscoelasticity

Experimental data on non-linear viscoelastic phenomena is available for two classes of aqueous system: CPyCl/NaSal [21], and CTAB/NaSal [14]. There appear to be several regimes of behaviour, even among systems that share the characteristic single-exponential stress decay in the linear regime. In some cases, there is significant departure from normal polymeric behaviour in non-linear flows, indicating a breakdown of either the assumption that the flow does not directly influence the reaction rates, or that non-polymeric stress contributions may be neglected (see section 4.4 above). For
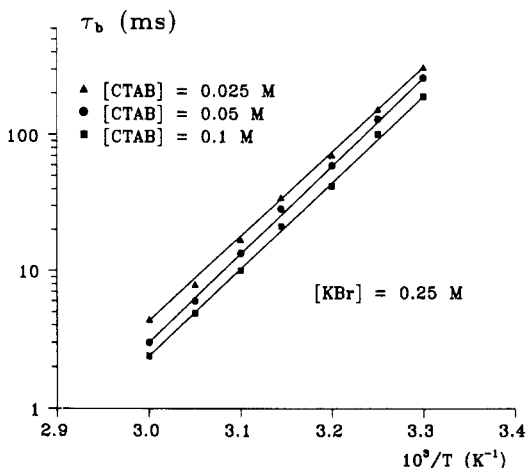
Figure 13. Variations of the breaking time τ_{break} as a function of $10^3/T$ for CTAB–0.25 M KBr solutions.

CPyCl/NaSal the stress optical law appears to be obeyed [14], which suggests failure of the first assumption rather than the second. Further detailed experiments will be needed to elucidate the full range of flow behaviours for worm-like micellar systems.

6. Conclusions

There is substantial experimental evidence that the viscoelastic phases seen in certain surfactant solutions (at a few weight per cent of amphiphile) contain large one-dimensional aggregates that can be regarded as equilibrium polymers. When excluded volume interactions are strong, the static chain conformations are in qualitative agreement with scaling predictions, based on the assumption that no closed rings are present. This assumption may be appropriate for micellar systems in which the polymeric repeat unit is large compared to a solvent molecule [37]. In regimes of weak excluded volume, mean-field exponents should be expected instead, and there is some evidence for this in suitable systems. Thus, most of the evidence from static correlations, as determined by scattering and other techniques, suggests that these viscoelastic surfactant solutions may indeed be regarded as equilibrium polymers [64].

A version of the reptation model, extended as described in section 4.2 to include the effect of reversible breakage, appears to offer a promising framework for understanding both self-diffusion [9] and linear viscoelastic measurements [56, 21, 14] on entangled worm-like micellar systems. It offers a plausible and robust explanation for the observed single-exponential relaxation spectrum. Other predictions, such as the concentration and temperature dependence of the relaxation time, are less clearly confirmed experimentally, although many of the results are consistent, at least for the CTAB/KBr system at high enough salt. The data suggest that salt concentration (in CTAB/KBr at low salt) and specific counterion effects (involving Sal^-, in systems that contain it) are important in determining the dependence of average micellar size on concentration and this complicates the interpretation for several of the other systems that have been studied experimimentally. We should also point out that the dilution behaviour and temperature dependence is complicated by the existence of various different regimes according to the chemical kinetic scheme, ratio of τ_{break} to

τ_{rep}, etc; several of these regimes [58–60] have not been touched on in the present article due to lack of space. Although the linear stress relaxation behaviour of these worm-like micellar systems is exceptionally simple (a near-perfect Maxwell fluid), the same cannot be said of non-linear viscoelastic phenomena, whose explanation remains a challenge for future theoretical and experimental studies.

Acknowledgments

References

[1] Porte G, Appell J and Poggi Y 1980 *J. Phys. Chem.* **84** 3105
[2] Porte G and Appell J 1981 *J. Phys. Chem.* **85** 2511
[3] Appell J and Porte G 1981 *J. Colloid Interface Sci.* **81** 85
[4] Appell J, Porte G and Poggi Y 1981 *J. Colloid Interface Sci.* **87** 492
[5] Porte G, Marignan J, Bassereau P and May R 1988 *J. Physique* **49** 511
[6] Candau S J, Hirsch E and Zana R 1984 *J. Physique* **45** 1263
[7] Candau S J, Hirsch E and Zana R 1985 *J. Colloid Interface Sci.* **105** 521
[8] Makhloufi R, Hirsch E, Candau S J, Binana-Limbele W and Zana R 1990 *J. Phys. Chem.* **94** 387
[9] Messager R, Ott A, Chatenay D, Urbach W and Langevin D 1988 *Phys. Rev. Lett.* **60** 1410
[10] Ikeda S, Ozeki S and Tsunoda M 1980 *J. Colloid Interface Sci.* **73** 27
[11] Ikeda S, Hayashi S and Imae T 1980 *J. Phys. Chem.* **84** 744
[12] Imae T, Kamiya R, Ikeda S 1985 *J. Colloid Interface Sci.* **108** 215
[13] Shikata T, Hirata H and Kotaka T 1987 *Langmuir* **3** 1081
Shikata T, Hirata H and Kotaka T 1988 *Langmuir* **4** 354
[14] Shikata T, Hirata H, Takatori E and Osaki K 1988 *J. Non-Newtonian Fluid Mech.* **28** 171
[15] Thurn H, Kalus J and Hoffmann H 1984 *J. Phys. Chem.* **80** 3440
[16] Hoffmann H, Kalus J, Thurn H and Ibel K 1983 *Ber. Bunsenges. Phys. Chem.* **87** 1120
[17] Kalus J, Hoffmann H, Reizlein K and Ulbricht W 1982 *Ber. Bunsenges. Phys. Chem.* **86** 37
[18] Hoffmann H, Lobl M and Rehage H 1985 *Physics of Amphiphiles: Micelles, Vesicles and Microemulsions* ed V Degiorgio and M Corti (Amsterdam: North Holland) p 237
[19] Hoffmann H, Loebl M, Rehage H and Wunderlich I 1986 *Tenside Detergents* **22** 290
[20] Hoffmann H, Rehage H and Wunderlich I 1987 *Rheol. Acta* **26** 532
[21] Rehage H and Hoffmann H 1988 *J. Phys. Chem.* **92** 4712
[22] Scartazzini R and Luisi P L 1988 *J. Phys. Chem.* **92** 829
[23] Schurtenberger P, Scartazzini R, Magid L J, Leser M E and Luisi P L 1990 *J. Phys. Chem.* **94** 3695
[24] Israelachvili J N, Mitchell D and Ninham B 1976 *J. Chem. Soc. Faraday Trans. II* **72** 1525
[25] Safran S A, Turkevich L and Pincus F 1984 *J. Physique Lett.* **45** L19
[26] Mukerjee P 1972 *J. Phys. Chem.* **76** 565
[27] Porte G, Appell J 1983 *Surfactants in Solution* vol 2, ed K L Mittal and B Lindman (New York: Plenum) p 805
[28] Blanckschtein D, Thurston G M and Benedek G B 1986 *Phys. Rev. Lett.* **54** 955
Blanckschtein D, Thurston G M and Benedek G B 1986 *J. Phys. Chem.* **85** 7268

[29] de Gennes P G 1979 *Scaling Concepts in Polymer Physics* (Ithaca, NY: Cornell University Press)

[30] Doi M and Edwards S F 1986 *The Theory of Polymer Dynamics* (Oxford: Clarendon)

[31] Worsfold D J and Bywater S 1957 *J. Polym. Sci.* **26** 299

[32] Bacon R F and Fanelli R 1943 *J. Am. Chem. Soc.* **65** 639
Gee G 1952 *Trans. Faraday. Soc.* **48** 515
Tobolsky A V and Eisenberg A 1959 *J. Am. Chem. Soc.* **81** 780

[33] Cates M E 1987 *Europhys. Lett.* **4** 497

[34] Faivre G and Gardissat J-L 1986 *Macromolecules* **19** 1988

[35] Scott R L 1965 *J. Phys. Chem.* **69** 261

[36] Petscheck R G Pfeuty P and Wheeler J C 1986 *Phys. Rev.* A **34** 2391
Kennedy S J and Wheeler J C 1983 *J. Phys. Chem.* **78** 953
Corrales L R and Wheeler J C 1989 *J. Phys. Chem.* **90** 5030

[37] Cates M E 1990 unpublished

[38] Safran S A, Pincus F Y L, Cates M E and MacKintosh F C 1990 *J. Physique* **51** 503

[39] Cates M E 1988 *J. Physique* **49** 1593

[40] Lang J and Zana R 1987 *Surfactant Solutions* ed R Zana (New York: Dekker) p 405 and references therein

[41] Anacker E W and Ghose H M 1968 *J. Am. Chem. Soc.* **90** 3161

[42] Mazer N A, Carey M C and Benedek G B 1977 *Proc. Int. Symp.* **1** 359

[43] Missel P J, Mazer N A, Benedek G B, Young C Y and Carey M 1980 *J. Phys. Chem.* **84** 1044

[44] Young C Y, Missel P J, Mazer N A, Benedek G B and Carey M C 1978 *J. Phys. Chem.* **82** 1375

[45] Missel P J, Mazer N A, Benedek G B and Carey M C 1982 *Solution Behavior of Surfactants* vol 1, ed E J Fendler and K L Mittal (New York: Plenum Press) p 1264

[46] Missel P J, Mazer N A, Benedek G B and Carey M C 1983 *J. Phys. Chem.* **87** 1264

[47] Van de Sande W and Persoons A 1985 *J. Phys. Chem.* **89** 404

[48] Hoffmann H, Kalus J, Reizlein K, Ulbricht W and Ibel K 1982 *Colloid Polym. Sci.* **260** 435

[49] Herbst L, Hoffmann H, Kalus J, Thurn H, Ibel K and May R P 1986 *J. Chem. Phys.* **103** 437

[50] Quirion F and Magid L 1986 *J. Phys. Chem.* **90** 5435

[51] Porte G 1989 private communication

[52] Hirsch E, Candau S J and Zana R 1986 *Surfactants in Solution* vol 4, ed K L Mittal and P Bothorel (New York: Plenum Press) p 317

[53] A somewhat more complex behaviour, as yet unexplained, was found by Brown W, Johansson K and Almgren M 1989 *J. Phys. Chem.* **93** 5888, in semi-dilute solutions of CTAB–naphthalene sodium. The autocorrelation function of the scattered intensity was found to be bimodal. The fast mode was diffusive, the diffusion constant varying as $\phi^{0.27}$. The relaxation time associated with the slower mode was q-independent and varied as $\phi^{-1.9}$.

[54] Schaeffer D W, Joanny J F and Pincus P 1980 *Macromolecules* **13** 1280

[55] Kern F, Collin D and Candau S J 1990 to be published

[56] Candau S J, Hirsch E, Zana R and Adam M 1988 *J. Colloid Interface Sci.* **122** 430

[57] Candau S J, Hirsch E, Zana R and Delsanti M 1989 *Langmuir* **5** 1525

[58] Cates M E 1987 *Macromolecules* **20** 2289

[59] Cates M E 1989 *Space–Time Organization in Macromolecular Fluids (Springer Series in Chemical Physics 51)* ed F Tanaka, M Doi and T Ohta p 116

[60] Cates M E 1990 *J. Phys. Chem.* **94** 371

[61] McLeish T C B and Cates M E unpublished

[62] Turner M S and Cates M E 1990 *J. Physique* **51** 307

[63] Candau S J, Merikhi F, Waton G and Lemaréchal P 1990 *J. Physique* **51** 977

[64] For a very recent further study, see: Appell J and Porte G 1990 *Europhys Lett.* **12** 185